VV precision predictions – Vector boson pair production at hadron colliders at NNLO QCD

Stefan Kallweit[1]

based on work with: F. Cascioli[b], T. Gehrmann[bc], M. Grazzini[a−f], P. Maierhöfer[bc], A. v. Manteuffel[bc], S. Pozzorini[bc], D. Rathlev[a−f], L. Tancredi[bc], A. Torre[a], E. Weihs[b], M. Wiesemann[e]

[f] arXiv:1507.06257 [hep-ph]
[e] arXiv:1507.02565 [hep-ph] (accepted for publication in JHEP)
[d] JHEP 1507 (2015) 085 [arXiv:1504.01330 [hep-ph]]
[c] Phys.Rev.Lett. 113 (2014) 21, 212001 [arXiv:1408.5243 [hep-ph]]
[b] Phys.Lett. B735 (2014) 311-313 [arXiv:1405.2219 [hep-ph]]
[a] Phys.Lett. B731 (2014) 204-207 [arXiv:1309.7000 [hep-ph]]

[1]University of Mainz

Aug 31–Sep 5, 2015, The Third Annual Large Hadron Collider Physics Conference
St. Petersburg, Russia

Outline

1. Introduction
2. Calculation of NNLO QCD cross sections with q_{T} subtraction
   - Idea of the q_{T} subtraction method
   - Implementation in the MATRIX framework
3. Numerical results at NNLO QCD and comparison to data
   - NNLO QCD results for $\mathrm{pp}(\to \mathrm{V}\gamma) \to \ell\ell\gamma/\ell\nu\gamma/\nu\nu\gamma + \mathrm{X}$
   - NNLO QCD results for $\mathrm{pp} \to \mathrm{W}^+\mathrm{W}^- + \mathrm{X}$
   - NNLO QCD results for $\mathrm{pp}(\to \mathrm{ZZ}) \to 4\ell + \mathrm{X}$
4. Conclusions & Outlook

Importance of going beyond NLO in QCD in VV production

Fully exclusive NNLO QCD calculations desirable for several reasons

- Experimental accuracy has significantly increased.
- A reduction of the unphysical dependence on factorization and renormalization scales — and in particular reliability of the remaining scale-variation uncertainty as an estimate for missing higher orders — is expected at NNLO.
  - In many process classes, all partonic channels are included only from NNLO on.
  - In some phase-space regions, NLO is the first non-vanishing order.
  - Jets are treated more realistically.

On the same expected order of magnitude (by naive counting of coupling constants), NLO EW corrections should also be taken into account.

Importance of VV production (with leptonic decays) at NNLO QCD

- Important Standard Model test $\rightarrow$ trilinear gauge-boson couplings.
- Background for Higgs analyses and BSM searches.
- Some moderate excesses ($\approx 2\sigma$) in experimental data compared to NLO prediction, e.g. $\mathrm{W}\gamma$ (ATLAS, 7 TeV), WW (ATLAS, 8 TeV; milder excess also seen at CMS).

Overview of the q_T subtraction method

Consider the production of a **colourless final state F** via $\mathbf{q\bar{q} \to F}$ or $\mathbf{gg \to F}$:

$$\mathrm{d}\sigma_{\mathrm{F}}^{\mathrm{(N)NLO}}\Big|_{q_\mathrm{T}\neq 0} = \mathrm{d}\sigma_{\mathrm{F+jet}}^{\mathrm{(N)LO}},$$

where q_T refers to the transverse momentum of the colourless system F. [Catani, Grazzini (2007)]

$\mathrm{d}\sigma_{\mathrm{F}}^{\mathrm{(N)NLO}}\Big|_{q_\mathrm{T}\neq 0}$ is singular for $q_T \to 0$, but the limiting behaviour is known from transverse momentum resummation. [Bozzi, Catani, de Florian, Grazzini (2006)]

- Define a universal counterterm with the complementary $q_T \to 0$ behaviour,
  $\mathrm{d}\sigma^{\mathrm{CT}} = \Sigma(q_T/m_F) \otimes \mathrm{d}\sigma^{\mathrm{LO}}$, with Σ known up to NNLO. [Bozzi, Catani, de Florian, Grazzini (2006)]
- $\mathrm{d}\sigma_{\mathrm{F+jet}}^{\mathrm{NLO}}$ can be treated by any local NLO subtraction technique, e.g. by conventional dipole subtraction. [Catani, Seymour (1993)]
- Add the $q_T = 0$ piece with the hard–collinear coefficient $\mathcal{H}_F$, which is derived from the 1-(2-)loop amplitudes in a process-independent way. [Catani, Cieri, de Florian, Ferrera, Grazzini (2013)]

↪ **Full result for (N)NLO cross section**

$$\mathrm{d}\sigma_{\mathrm{F}}^{\mathrm{(N)NLO}} = \mathcal{H}_{\mathrm{F}}^{\mathrm{(N)NLO}} \otimes \mathrm{d}\sigma^{\mathrm{LO}} + \left[\mathrm{d}\sigma_{\mathrm{F+jet}}^{\mathrm{(N)LO}} - \Sigma^{\mathrm{(N)NLO}} \otimes \mathrm{d}\sigma^{\mathrm{LO}}\right]_{\mathrm{cut}_{q_T}\to 0}$$

External ingredients: amplitudes applied in the calculation

Scattering amplitudes up to 1-loop with OPENLOOPS [Cascioli, Maierhöfer, Pozzorini (2011); Cascioli, Lindert, Maierhöfer, Pozzorini (2014)]

- Tree, one-loop and real-emission amplitudes (including colour/helicity correlations)
- Provides also finite (1-loop)-squared amplitudes (not only)
- Fully automated for NLO (QCD+EW) for any SM process
- Compact and fast numerical code

Tensor reduction by means of the COLLIER library [Denner, Dittmaier, Hofer (2014)]

- Numerically stable Denner–Dittmaier reduction methods [Denner, Dittmaier (2002 & 2005)]
- Scalar integrals with complex masses [Denner, Dittmaier (2010)]

Rescue system by quad-precision CUTTOOLS for critical points [Ossola, Papadopoulos, Pittau (2008)]

- Scalar integrals from ONELOOP [van Hameren, Papadopoulos, Pittau (2009); van Hameren (2010)]

2-loop amplitudes from analytic results

- Drell–Yan-like amplitudes from [Matsuura, van der Marck, van Neerven (1989)]
- $V\gamma$ helicity amplitudes from [Gehrmann, Tancredi (2011)], using TDHPL [Gehrmann, Remiddi (2001)]
- On-shell VV amplitudes from private code [von Manteuffel, Tancredi (2014)], using GINAC (applied in [Cascioli et al. (2014); Gehrmann et al. (2014); Grazzini, SK, Rathlev, Wiesemann (2015)])
- Off-shell helicity VV' amplitudes from VVAMP [Gehrmann, von Manteuffel, Tancredi (2015)], using GINAC [Bauer, Frink, Kreckel (2002) + Kisil, Sheplyakov, Vollinga, …] (independent calculation by [Caola, Henn, Melnikov, Smirnov, Smirnov (2014)])

The MATRIX framework for automated NNLO+NNLL calculations

Amplitudes

OPENLOOPS	Dedicated 2-loop codes
(COLLIER, CUTTOOls, ...)	(VVAMP, GINAC, TDHPL, ...)

MUNICH

MUlti-cha**N**nel **I**ntegrator at Swiss (**CH**) precision

q_T subtraction $\Leftrightarrow$ q_T resummation

NNLO

NNLL

MATRIX

MUNICH **A**utomates q**T** Subtraction
and **R**esummation to **I**ntegrate **X**-sections.

Fiducial cross sections for $\mathrm{pp}(\to \mathrm{V}\gamma) \to \ell\ell\gamma/\ell\nu\gamma/\nu\nu\gamma + \mathrm{X}$

Setup adapted to the ATLAS analysis @ 7 TeV [ATLAS collaboration (2013)]

process	$p_{\mathrm{T,cut}}^{\gamma}$	N_{jet}	σ_{LO} [pb]	σ_{NLO} [pb]	σ_{NNLO} [pb]	σ_{ATLAS} [pb]	$\frac{\sigma_{\mathrm{NLO}}}{\sigma_{\mathrm{LO}}}$	$\frac{\sigma_{\mathrm{NNLO}}}{\sigma_{\mathrm{NLO}}}$
$\mathbf{Z}\gamma \to \ell\ell\gamma$	soft	≥ 0	$0.8149\,^{+8.0\%}_{-9.3\%}$	$1.222\,^{+4.2\%}_{-5.3\%}$	$1.320\,^{+1.3\%}_{-2.3\%}$	1.31 ±0.02 (stat) ±0.11 (syst) ±0.05 (lumi)	+50%	+8%
		$= 0$		$1.031\,^{+2.7\%}_{-4.3\%}$	$1.059\,^{+0.7\%}_{-1.4\%}$	1.05 ±0.02 (stat) ±0.10 (syst) ±0.04 (lumi)	+27%	+3%
	hard	≥ 0	$0.0736\,^{+3.4\%}_{-4.5\%}$	$0.1320\,^{+4.2\%}_{-4.0\%}$	$0.1543\,^{+3.1\%}_{-2.8\%}$		+79%	+17%
$\mathbf{Z}\gamma \to \nu\nu\gamma$		≥ 0	$0.0788\,^{+0.3\%}_{-0.9\%}$	$0.1237\,^{+4.1\%}_{-3.1\%}$	$0.1380\,^{+2.5\%}_{-2.3\%}$	0.133 ±0.013 (stat) ±0.020 (syst) ±0.005 (lumi)	+57%	+12%
		$= 0$		$0.0881\,^{+1.2\%}_{-1.3\%}$	$0.0866\,^{+1.0\%}_{-0.9\%}$	0.116 ±0.010 (stat) ±0.013 (syst) ±0.004 (lumi)	+12%	−2%
$\mathbf{W}\gamma \to \ell\nu\gamma$	soft	≥ 0	$0.8726\,^{+6.8\%}_{-8.1\%}$	$2.058\,^{+6.8\%}_{-6.8\%}$	$2.453\,^{+4.1\%}_{-4.1\%}$	2.77 ±0.03 (stat) ±0.33 (syst) ±0.14 (lumi)	+136%	+19%
		$= 0$		$1.395\,^{+5.2\%}_{-5.8\%}$	$1.493\,^{+1.7\%}_{-2.7\%}$	1.76 ±0.03 (stat) ±0.21 (syst) ±0.08 (lumi)	+60%	+7%
	hard	≥ 0	$0.1158\,^{+2.6\%}_{-3.7\%}$	$0.3959\,^{+9.0\%}_{-7.3\%}$	$0.4971\,^{+5.3\%}_{-4.7\%}$		+242%	+26%

- Loop-induced gg contributions in $\mathrm{Z}\gamma$ turn out to be very small ($<$ 15% of NNLO).
- Larger K factors in $\mathrm{W}\gamma$ than in $\mathrm{Z}\gamma$ can be explained by breaking of radiation zero.
- Larger K factors in hard wrt. soft setups due to implicit phase-space restrictions …

Invariant/transverse mass distributions for $\mathrm{pp} \to \ell\ell\gamma/\ell\nu\gamma + \mathrm{X}$

$\mathbf{pp}\ (\to \mathbf{Z}\gamma) \to \ell\ell\gamma + \mathbf{X}$ Distribution in the invariant mass $m_{\ell\ell\gamma}$

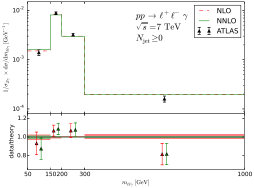

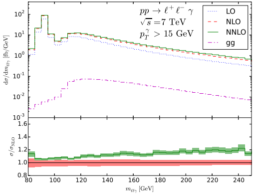

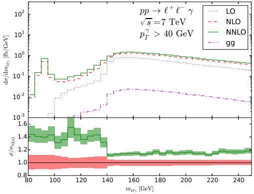

- Implicit LO phase-space restrictions: $m_{\ell\ell\gamma} \approx 66\,\mathrm{GeV}$ (soft) vs. $m_{\ell\ell\gamma} \approx 97\,\mathrm{GeV}$ (hard)

$\mathbf{pp}\ (\to \mathbf{W}\gamma) \to \ell\nu\gamma + \mathbf{X}$ Distribution in the transverse mass $m_{\mathrm{T}}^{\ell\nu\gamma}$

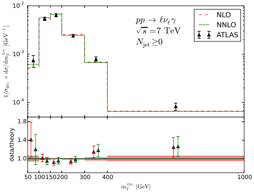

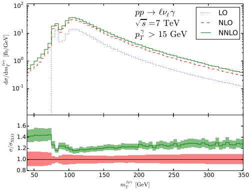

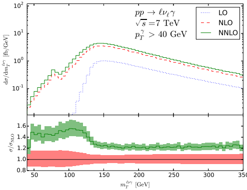

- Implicit LO phase-space restrictions: $m_{\mathrm{T}}^{\ell\nu\gamma} \approx 75\,\mathrm{GeV}$ (soft) vs. $m_{\mathrm{T}}^{\ell\nu\gamma} \approx 100\,\mathrm{GeV}$ (hard)

p_T^γ distributions for $\mathrm{pp}(\rightarrow \mathrm{Z}\gamma/\mathrm{W}\gamma) \rightarrow \ell\ell\gamma/\ell\nu\gamma + \mathrm{X}$

Distribution in the transverse momentum of the photon p_T^γ

$\mathbf{pp}\ (\rightarrow \mathbf{Z}\gamma) \rightarrow \ell\ell\gamma + \mathbf{X}$

$N_\mathrm{jet} \geq 0$ (left)
$N_\mathrm{jet} = 0$ (right)

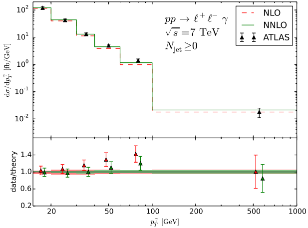

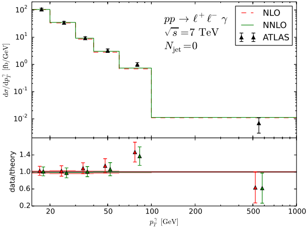

$\mathbf{pp}\ (\rightarrow \mathbf{W}\gamma) \rightarrow \ell\nu\gamma + \mathbf{X}$

$N_\mathrm{jet} \geq 0$ (left)
$N_\mathrm{jet} = 0$ (right)

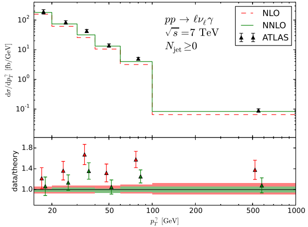

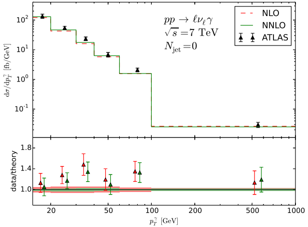

- Agreement between data and theory is significantly improved when including NNLO corrections as compared to NLO prediction, in particular without jet veto.

Inclusive on-shell WW cross sections for relevant LHC energies

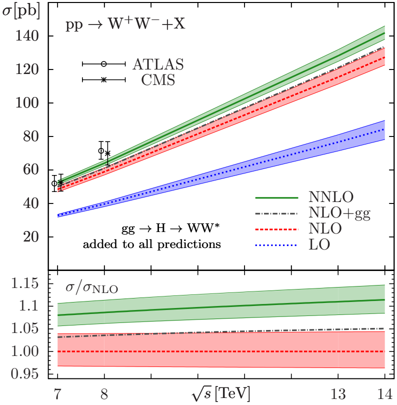

$\sqrt{s}$ [TeV]	σ_{LO} [pb]	σ_{NLO} [pb]	σ_{NNLO} [pb]	$\sigma_{gg\to H\to WW^*}$ [pb]
7	$29.52^{+1.6\%}_{-2.5\%}$	$45.16^{+3.7\%}_{-2.9\%}$	$49.04^{+2.1\%}_{-1.8\%}$	$3.25^{+7.1\%}_{-7.8\%}$
8	$35.50^{+2.4\%}_{-3.5\%}$	$54.77^{+3.7\%}_{-2.9\%}$	$59.84^{+2.2\%}_{-1.9\%}$	$4.14^{+7.2\%}_{-7.8\%}$
13	$67.16^{+5.5\%}_{-6.7\%}$	$106.0^{+4.1\%}_{-3.2\%}$	$118.7^{+2.5\%}_{-2.2\%}$	$9.44^{+7.4\%}_{-7.9\%}$
14	$73.74^{+5.9\%}_{-7.2\%}$	$116.7^{+4.1\%}_{-3.3\%}$	$131.3^{+2.6\%}_{-2.2\%}$	$10.64^{+7.5\%}_{-8.0\%}$

- Scale uncertainties at NNLO about $\pm 3\%$ ($M_W/2 < \mu_R, \mu_F < 2M_W$, $1/2 < \mu_R/\mu_F < 2$).
- Loop-induced gg channel provides about 35% of NNLO effect.
- NNLO/NLO ranges from 9% to 12% when $\sqrt{s}$ varies from 7 TeV to 14 TeV.

- 2σ excess in ATLAS 8TeV data is clearly reduced by positive NNLO corrections.
- Further corrections should be taken into account: • off-shell effects • EW corrections • photon-induced contributions • NLO QCD for loop-induced gg channel • ...
- Calculation of fiducial cross sections could circumvent possible extrapolation problems.

On-shell WW cross section and p_T-veto efficiencies with resummation

Relevant for extrapolation from fiducial to inclusive cross section:

p_T-veto efficiency

$$\epsilon(p_T^{\text{veto}}) = \sigma(p_T < p_T^{\text{veto}})/\sigma_{\text{tot}} \,.$$

The p_T-veto efficiency considered here refers to the transverse momentum of the WW system; it is not the jet-veto efficiency.

However, the two transverse momenta are clearly correlated (and coincide up to $\mathcal{O}(\alpha_s)$).

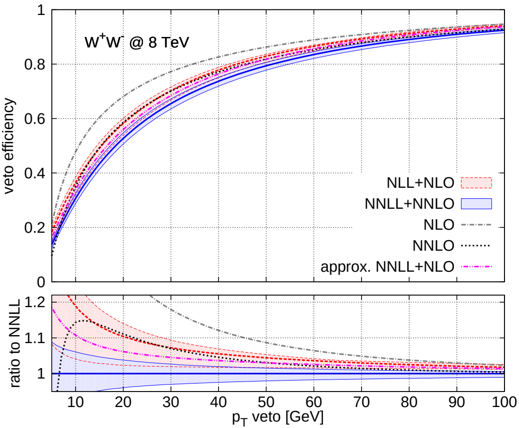

- In the relevant range of $p_T^{\text{veto}} \sim 25 - 30$ GeV, the approx. NNLL+NLO prediction (used in the latest CMS WW measurement [CMS collaboration (2015)] , which is in good agreement with NNLO prediction) is between NNLO and NNLL+NNLO (best) prediction, but still $\approx 5\%$ higher than NNLL+NNLO ($\approx 3\%$ higher p_T-veto efficiency).

Inclusive on-shell ZZ cross sections for relevant LHC energies

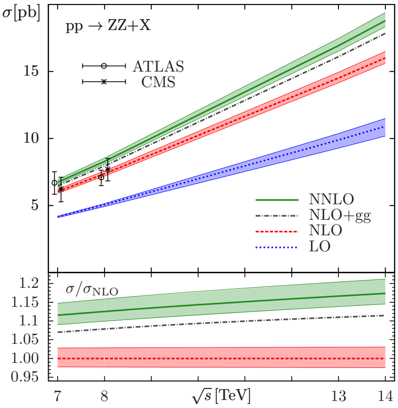

$\sqrt{s}$ [TeV]	σ_{LO} [pb]	σ_{NLO} [pb]	σ_{NNLO} [pb]
7	$4.172^{+0.7\%}_{-1.6\%}$	$6.049^{+2.8\%}_{-2.2\%}$	$6.747^{+2.9\%}_{-2.3\%}$
8	$5.066^{+2.7\%}_{-1.6\%}$	$7.376^{+2.8\%}_{-2.3\%}$	$8.294^{+3.0\%}_{-2.3\%}$
13	$9.899^{+4.9\%}_{-6.1\%}$	$14.52^{+3.0\%}_{-2.4\%}$	$16.93^{+3.3\%}_{-2.4\%}$
14	$10.92^{+5.4\%}_{-6.7\%}$	$16.02^{+3.0\%}_{-2.4\%}$	$18.80^{+3.3\%}_{-2.4\%}$

- Scale uncertainties at NNLO about $\pm 3\%$ ($M_{\mathrm{Z}}/2 < \mu_{\mathrm{R}}, \mu_{\mathrm{F}} < 2M_{\mathrm{Z}}$, $1/2 < \mu_{\mathrm{R}}/\mu_{\mathrm{F}} < 2$).
- Loop-induced gg channel provides about 60% of NNLO effect.
- NNLO/NLO ranges from 12% to 17% when $\sqrt{s}$ varies from 7 TeV to 14 TeV.
- LO, NLO, and NNLO bands don't overlap → underestimation of missing higher orders.
- No electroweak corrections included.
- Resonant ZZ contributions are experimentally isolated by $m_{\ell\ell}$ cuts.
  ↪ Cross sections are slightly overestimated in on-shell calculation.

Fiducial off-shell cross sections for $\mathrm{pp}(\to \mathrm{ZZ}) \to 4\ell + \mathrm{X}$

Setup adapted to the ATLAS analysis @ 8 TeV [ATLAS collaboration (2013)]

channel	σ_{LO} [fb]	σ_{NLO} [fb]	σ_{NNLO} [fb]	σ_{ATLAS} [fb]
$e^+e^-e^+e^-$	$3.547(1)^{+2.9\%}_{-3.9\%}$	$5.047(1)^{+2.8\%}_{-2.3\%}$	$5.79(2)^{+3.4\%}_{-2.6\%}$	$4.6^{+0.8}_{-0.7}(\mathrm{stat})^{+0.4}_{-0.4}(\mathrm{syst})^{+0.1}_{-0.1}(\mathrm{lumi})$
$\mu^+\mu^-\mu^+\mu^-$				$5.0^{+0.6}_{-0.5}(\mathrm{stat})^{+0.2}_{-0.2}(\mathrm{syst})^{+0.2}_{-0.2}(\mathrm{lumi})$
$e^+e^-\mu^+\mu^-$	$6.950(1)^{+2.9\%}_{-3.9\%}$	$9.864(2)^{+2.8\%}_{-2.3\%}$	$11.31(2)^{+3.2\%}_{-2.5\%}$	$11.1^{+1.0}_{-0.9}(\mathrm{stat})^{+0.5}_{-0.5}(\mathrm{syst})^{+0.3}_{-0.3}(\mathrm{lumi})$

- Agreement significantly improved in different-flavour channel.
- Worse agreement in same-flavour channels, but still consistent at the $\approx 1\sigma$ level.

Setup adapted to the CMS analysis @ 8 TeV [CMS collaboration (2015)]

channel	σ_{LO} [fb]	σ_{NLO} [fb]	σ_{NNLO} [fb]
$e^+e^-e^+e^-$	$3.149(1)^{+3.0\%}_{-4.0\%}$	$4.493(1)^{+2.8\%}_{-2.3\%}$	$5.16(1)^{+3.3\%}_{-2.6\%}$
$\mu^+\mu^-\mu^+\mu^-$	$2.973(1)^{+3.1\%}_{-4.1\%}$	$4.255(1)^{+2.8\%}_{-2.3\%}$	$4.90(1)^{+3.4\%}_{-2.6\%}$
$e^+e^-\mu^+\mu^-$	$6.179(1)^{+3.1\%}_{-4.0\%}$	$8.822(1)^{+2.8\%}_{-2.3\%}$	$10.15(2)^{+3.3\%}_{-2.6\%}$

- No fiducial cross sections provided by CMS, but normalized distributions ...

Normalized distributions for off-shell $\mathrm{pp}(\to \mathrm{ZZ}) \to 4\ell + \mathrm{X}$ production

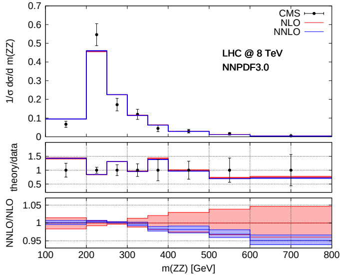

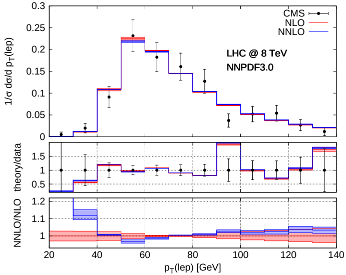

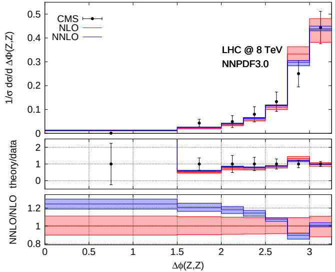

- $m(\mathrm{ZZ})$ and $p_{\mathrm{T}}^{\mathrm{lep}}$ distributions
  - No significant NNLO impact on the data–theory comparison of shapes.
  - The NNLO effect on shapes is dominated by the gluon-fusion contribution.
- For the $\Delta\phi(\mathrm{ZZ})$ distribution, the NNLO corrections improve the agreement with data ($\Delta\phi(\mathrm{ZZ}) = \pi$ in LO kinematics).

Conclusions & Outlook

Conclusions

- MATRIX – an automated framework to perform fully differential NNLO (+NNLL) QCD computations for colourless final-state production, based on MUNICH and q_{T} subtraction (+resummation), applying OPENLOOPS and dedicated 2-loop amplitudes.
- NNLO QCD results calculated in the MATRIX framework
  ↪ Improved agreement between data and theory by NNLO prediction.
  - Fully differential results for $\mathrm{pp}(\to \mathrm{V}\gamma) \to \ell\ell\gamma/\ell\nu\gamma/\nu\nu\gamma + \mathrm{X}$
    - NLO and NNLO corrections for $\mathrm{W}\gamma$ much larger than for $\mathrm{Z}\gamma$ (radiation zero).
    - NNLO corrections up to $\approx 25\%$ (gg contribution in $Z\gamma$ very small).
  - Inclusive cross sections for $\mathrm{pp} \to \mathrm{W}^+\mathrm{W}^- + \mathrm{X}$
    - NNLO corrections of $\approx 10\%$ (gg contribution $\approx 35\%$ thereof).
    - NNLL+NNLO studies to assess the effect on the p_{T}-veto efficiency.
  - Fully differential results for $\mathrm{pp}(\to \mathrm{ZZ}) \to 4\ell + \mathrm{X}$
    - NNLO corrections of $\approx 15\%$ (gg contribution $\approx 60\%$ thereof).

Outlook

- Combination with NLO EW corrections, studies on pdf uncertainties, . . .
- More phenomenological studies on NNLO effects on vector-boson pair production.
- Medium-term goal: Public version of the numerical program MATRIX.

Backup

Backup slides

Comparison between $\mathrm{Z}\gamma$ and $\mathrm{W}\gamma$ results

Considerably larger K factors in Wγ than in Zγ

process	$p_{\mathrm{T,cut}}^{\gamma}$	N_{jet}	$\frac{\sigma_{\mathrm{NLO}}}{\sigma_{\mathrm{LO}}}$	$\frac{\sigma_{\mathrm{NNLO}}}{\sigma_{\mathrm{NLO}}}$
$Z\gamma$	soft	$N_{\mathrm{jet}} \geq 0$	$+50\%$	$+8\%$
$W\gamma$	soft	$N_{\mathrm{jet}} \geq 0$	$+136\%$	$+19\%$
$Z\gamma$	soft	$N_{\mathrm{jet}} = 0$	$+27\%$	$+3\%$
$W\gamma$	soft	$N_{\mathrm{jet}} = 0$	$+60\%$	$+7\%$
$Z\gamma$	hard	$N_{\mathrm{jet}} \geq 0$	$+79\%$	$+17\%$
$W\gamma$	hard	$N_{\mathrm{jet}} \geq 0$	$+242\%$	$+26\%$

Explanation: **Breaking of radiation zero beyond LO**

- $\mathrm{u\bar{d}/d\bar{u}} \to \mathrm{W}^{\pm}\gamma$ amplitudes vanish at $\cos\theta_{\mathrm{q}\gamma,\mathrm{CMS}} = \mp 1/3$. [Mikaelian/Samuel/Sahdev (1979)]
- Radiation zero leads to a dip at $\Delta \mathrm{y}_{\mathrm{l}\gamma} = 0$ in pp collisions. [Baur/Errede/Landsberg (1994)]

$\hookrightarrow$ Dip filled by higher-order corrections.

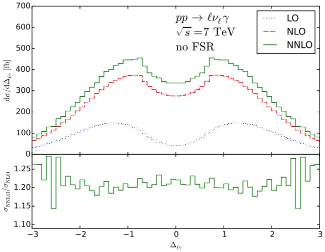

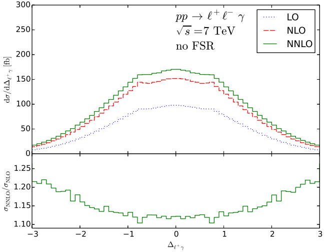

Numerical stability and dependence on $\mathrm{cut}_{q_\mathrm{T}/q}$

$\mathbf{q_T}$ subtraction at NLO

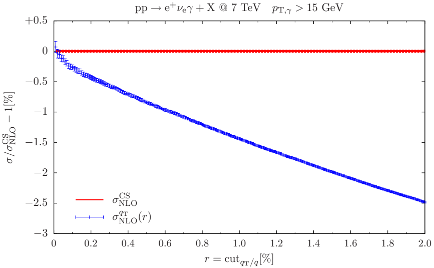

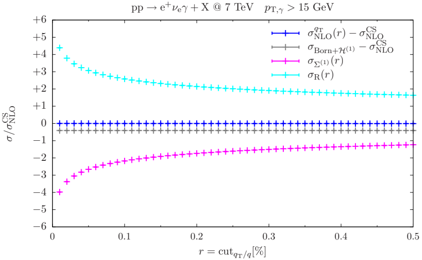

$\mathbf{q_T}$ subtraction at NNLO

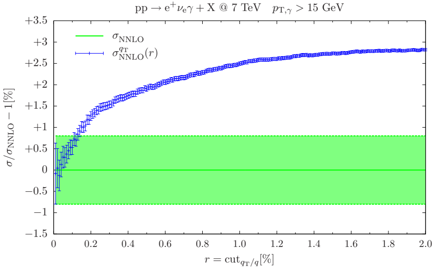

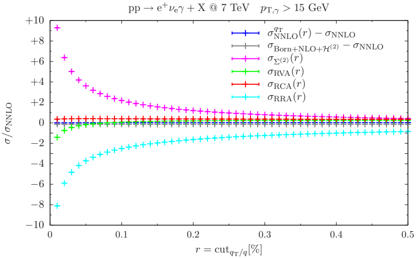

Photon isolation

Two contributions to photon production

- Direct production in the hard process,
- Non-perturbative fragmentation of a hard parton.

Different approaches to define isolated photons

- Naive ansatz: forbid any partons inside a fixed cone around the photon.
  $\hookrightarrow$ Not infrared safe beyond LO QCD as soft gluons inside the cone are forbidden.
- Hard cone isolation (experimentally preferred)

$$\sum_{\delta' < \delta_0} E_{\mathrm{had,T}}(\delta') \quad \leq \quad \varepsilon_\gamma E_{\gamma,\mathrm{T}}, \qquad\qquad \delta_{i\gamma} = \sqrt{(\eta_i - \eta_\gamma)^2 + (\phi_i - \phi_\gamma)^2}$$

  $\hookrightarrow$ Only infrared safe if combined with fragmentation contribution (due to quark–photon collinear singularity).
- **Smooth cone isolation** [Frixione (1998)]

$$\sum_{\delta' < \delta} E_{\mathrm{had,T}}(\delta') \quad \leq \quad \varepsilon_\gamma E_{\gamma,\mathrm{T}} \left(\frac{1 - \cos(\delta)}{1 - \cos(\delta_0)} \right)^n \quad \forall \quad \delta \leq \delta_0$$

  $\hookrightarrow$ Smooth cone isolation eliminates fragmentation contribution completely.

NLO QCD cross section via dipole subtraction

Schematic formula for the NLO cross section with dipoles [Catani, Seymour (1993)]:

$$\sigma^{\mathrm{NLO}} = \underbrace{\int_{m+1} d\sigma^R}_{\text{real corrections}} + \underbrace{\int_m d\sigma^V}_{\text{virtual corrections}} + \underbrace{\int_0^1 dz \int_m d\sigma^C}_{\text{collinear-subtraction counterterm}} - \int_{m+1} d\sigma^A + \int_{m+1} d\sigma^A,$$

$$d\sigma^A = \sum_{\mathrm{dipoles}} d\sigma^B \otimes dV_{\mathrm{dipole}}$$

$$= \int_{m+1} \left[d\sigma^R - d\sigma^A\right]_{\epsilon=0} \qquad \Rightarrow \mathrm{RA}$$

$$+ \int_m \left[d\sigma^V + \sum_{\mathrm{dipoles}} d\sigma^B \otimes V_{\mathrm{dipole}}(1)\right]_{\epsilon=0} \qquad \Rightarrow \mathrm{VA}$$

$$+ \int_0^1 dz \int_m \left[d\sigma^C + \sum_{\mathrm{dipoles}} \int_1 d\sigma^B(z) \otimes \left[dV_{\mathrm{dipole}}(z)\right]_+\right]_{\epsilon=0} \qquad \Rightarrow \mathrm{CA}$$

$$dV_{\mathrm{dipole}}(z) = \left[dV_{\mathrm{dipole}}(z)\right]_+ + dV_{\mathrm{dipole}}(1)\delta(1-z)$$

NLO QCD cross section via q_T subtraction

Schematic formula for the NLO cross section

$$\sigma^{\mathrm{NLO}} = \underbrace{\int_{m+1} d\sigma^R}_{\text{real}} + \underbrace{\int_m d\sigma^V}_{\text{virtual}} + \underbrace{\int_0^1 dz \int_m d\sigma^C}_{\text{collinear counterterm}}$$

$$= \int_{m+1} d\sigma^R \Big|_{q_\mathrm{T}/q > \mathrm{cut}_{q_\mathrm{T}/q}} \qquad \Rightarrow \text{finite, but depends on } \mathrm{cut}_{q_\mathrm{T}/q}$$

$$+ \underbrace{\int_{m+1} d\sigma^R \Big|_{q_\mathrm{T}/q \leq \mathrm{cut}_{q_\mathrm{T}/q}}}_{\substack{\text{approximated by results known} \\ \text{from } q_\mathrm{T} \text{ resummation}}} + \underbrace{\int_m d\sigma^V + \int_0^1 dz \int_m d\sigma^C}_{\substack{\text{identified with corresponding terms} \\ \text{in } q_\mathrm{T} \text{ resummation}}}$$

$$\approx \int_{m+1} d\sigma^R \Big|_{q_\mathrm{T}/q > \mathrm{cut}_{q_\mathrm{T}/q}} + \frac{\alpha_S}{\pi} \mathcal{H}^{F(1)} \otimes \sigma_{\mathrm{LO}}$$

- no $\mathrm{cut}_{q_\mathrm{T}/q}$ dependence,
- contains (finite) 1-loop part.

$$+ \frac{\alpha_S}{\pi} \int_{\mathrm{cut}_{q_\mathrm{T}/q}}^{\infty} d(q_\mathrm{T}/q) \Sigma^{(1)}(q_\mathrm{T}/q) \otimes \sigma_{\mathrm{LO}}$$

- cancels $\mathrm{cut}_{q_\mathrm{T}/q}$ dependence,
- assigned to Born phase-space.

NNLO QCD cross section via q_{T} subtraction

Schematic formula for the NNLO cross section

$$\sigma^{\mathrm{NNLO}} = \underbrace{\underbrace{\int_{m+2} d\sigma^{RR}}_{\text{double-real}} + \underbrace{\int_{m+1} d\sigma^{RV}}_{\text{real–virtual}} + \underbrace{\int_0^1 dz \int_{m+1} d\sigma^{RC}}_{\text{real–collinear}}}$$

$$= \sigma^{\mathrm{NLO}}_{F+jet} \quad \Rightarrow$$ at $q_{\mathrm{T}} \neq 0$ calculable via NLO subtraction, but divergent for $q_{\mathrm{T}} \to 0 \Rightarrow \mathrm{cut}_{q_{\mathrm{T}}/q}$

$$+ \underbrace{\int_m d\sigma^{VV}}_{\text{double-virtual}} + \underbrace{\int_0^1 dz \int_m d\sigma^{VC}}_{\text{virtual–collinear}} + \underbrace{\int_0^1 dz_1 \int_0^1 dz_2 \int_m d\sigma^{CC}}_{\text{double-collinear}}$$

$$= \sigma^{\mathrm{NLO}}_{F+jet}\Big|_{q_{\mathrm{T}}/q \,>\, \mathrm{cut}_{q_{\mathrm{T}}/q}}$$

$$+ \underbrace{\sigma^{\mathrm{NLO}}_{F+jet}\Big|_{q_{\mathrm{T}}/q \,\leq\, \mathrm{cut}_{q_{\mathrm{T}}/q}}}_{\substack{\text{approximated by results known}\\ \text{from } q_{\mathrm{T}} \text{ resummation}}} + \underbrace{\int_m d\sigma^{VV} + \int_0^1 dz \int_m d\sigma^{VC} + \int_0^1 dz_1 \int_0^1 dz_2 \int_m d\sigma^{CC}}_{\substack{\text{identified with corresponding terms}\\ \text{in } q_{\mathrm{T}} \text{ resummation}}}$$

NNLO QCD cross section via q_T subtraction

Schematic formula for the NNLO cross section

$$\sigma^{\mathrm{NNLO}} = \underbrace{\left[\int_{m+2} d\sigma^{RRA} + \int_{m+1} d\sigma^{RVA} + \int_0^1 dz \int_{m+1} d\sigma^{RCA}\right]\Bigg|_{q_\mathrm{T}/q\,>\,\mathrm{cut}_{q_\mathrm{T}/q}}}_{=\,\sigma^{\mathrm{NLO}}_{F+jet}\big|_{q_\mathrm{T}/q\,>\,\mathrm{cut}_{q_\mathrm{T}/q}}} \Rightarrow \text{ finite, but dependence on } \mathrm{cut}_{q_\mathrm{T}/q}$$

$$+\left(\frac{\alpha_S}{\pi}\right)^2 \mathcal{H}^{F(2)} \otimes \sigma_{\mathrm{LO}}$$

- no $\mathrm{cut}_{q_\mathrm{T}/q}$ dependence,
- contains (finite) 2-loop part.

$$+\left(\frac{\alpha_S}{\pi}\right)^2 \int_{\mathrm{cut}_{q_\mathrm{T}/q}}^{\infty} d(q_\mathrm{T}/q)\Sigma^{(2)}(q_\mathrm{T}/q) \otimes \sigma_{\mathrm{LO}}$$

- cancels $\mathrm{cut}_{q_\mathrm{T}/q}$ dependence,
- contains (finite) 1-loop part,
- assigned to Born phase-space.

All relevant ingredients from q_T resummation ($\mathcal{H}^{F(i)}$, $\Sigma^{(i)}(q_\mathrm{T}/q)$ for $i \leq 2$) are known.

$\hookrightarrow$ **Direct implementation into a Monte Carlo integrator feasible.**

Numerical realization of the calculation

Realized within the fully automated NLO (QCD+EW) Monte Carlo framework
MUNICH (MUlti-chaNnel Integrator at Swiss (CH) precision) [SK]

- Applicable for arbitrary Standard Model processes (including partonic bookkeeping).
- Phase-space integration by highly efficient multi-channel Monte Carlo techniques
  $\hookrightarrow$ Additional MC channels based on dipole kinematics constructed at runtime.
- OpenLoops interface, automatized implementation of dipole subtraction, etc.
- Simultaneous calculation for different scale choices and variations.

Extension to automated (q_T subtraction) NNLO QCD framework [Grazzini, SK, Rathlev]

- Process-independent construction of $\mathrm{cut}_{q_\mathrm{T}/q}$-dependent counterterms $\Sigma^{(1,2)}$.
- Process-independent extraction procedure for hard coefficients $\mathcal{H}^{(1,2)}$.
- NLO calculation for F+jet with finite $\mathrm{cut}_{q_\mathrm{T}/q}$ already available in Munich.
- Importance sampling performed on top of multi-channel approach
  $\hookrightarrow$ improved efficiency and reliability in particular for low $\mathrm{cut}_{q_\mathrm{T}/q}$ values.
- Simultaneous evaluation of observables for different values of the regulator $\mathrm{cut}_{q_\mathrm{T}/q}$
  $\hookrightarrow$ allows for monitoring of $\mathrm{cut}_{q_\mathrm{T}/q}$ and for extrapolation $\mathrm{cut}_{q_\mathrm{T}/q} \to 0$.

Numerical results for $\mathrm{pp} \to \mathrm{Z}\gamma \to \mathrm{l}^-\mathrm{l}^+\gamma + \mathrm{X}$ at NNLO QCD

Setup adapted to the ATLAS analysis @ 7 TeV

[ATLAS collaboration (2013)]

Leptons	$p_\mathrm{T}^\ell > 25\,\mathrm{GeV}$ $\lvert\eta^\ell\rvert < 2.47$
Photon	$p_\mathrm{T}^\gamma > 15\,\mathrm{GeV}$ (soft p_T^γ cut) or $p_\mathrm{T}^\gamma > 40\,\mathrm{GeV}$ (hard p_T^γ cut) $\lvert\eta^\gamma\rvert < 2.37$ Frixione isolation with $\varepsilon_\gamma = 0.5$, $R = 0.4$, $n = 1$
Jets	anti-k_T algorithm with $D = 0.4$ $p_\mathrm{T}^\mathrm{jet} > 30\,\mathrm{GeV}$ $\lvert\eta^\mathrm{jet}\rvert < 4.4$ $N_\mathrm{jet} \geq 0$ (inclusive) or $N_\mathrm{jet} = 0$ (exclusive)
Separation	$m_{\ell^+\ell^-} > 40\,\mathrm{GeV}$ $\Delta R(\ell, \gamma) > 0.7$ $\Delta R(\ell/\gamma, \mathrm{jet}) > 0.3$

LO diagrams

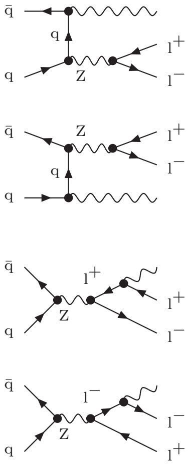

Numerical results for $\mathrm{pp} \to \mathrm{W}\gamma \to \mathrm{l}\nu\gamma + \mathrm{X}$ at NNLO QCD

Setup adapted to the ATLAS analysis @ 7 TeV

[ATLAS collaboration (2013)]

Lepton	$p_\mathrm{T}^\ell > 25\,\mathrm{GeV}$ $\lvert\eta\rvert < 2.47$
Neutrino	$p_\mathrm{T}^\nu > 35\,\mathrm{GeV}$
Photon	$p_\mathrm{T}^\gamma > 15\,\mathrm{GeV}$ (soft p_T^γ cut) or $p_\mathrm{T}^\gamma > 40\,\mathrm{GeV}$ (hard p_T^γ cut) $\lvert\eta^\gamma\rvert < 2.37$ Frixione isolation with $\varepsilon_\gamma = 0.5$, $R = 0.4$, $n = 1$
Jets	anti-k_T algorithm with $D = 0.4$ $p_\mathrm{T}^\mathrm{jet} > 30\,\mathrm{GeV}$ $\lvert\eta^\mathrm{jet}\rvert < 4.4$ $N_\mathrm{jet} \geq 0$ (inclusive) or $N_\mathrm{jet} = 0$ (exclusive)
Separation	$\Delta R(\ell, \gamma) > 0.7$ $\Delta R(\ell/\gamma, \mathrm{jet}) > 0.3$

LO diagrams

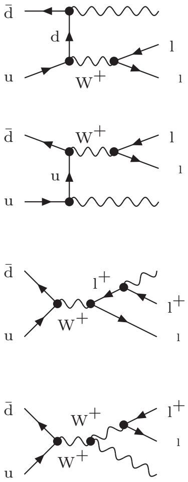

Numerical results for $\mathrm{pp} \to \mathrm{Z}\gamma \to \nu\bar{\nu}\gamma + \mathrm{X}$ at NNLO QCD

Setup adapted to the ATLAS analysis @ 7 TeV

[ATLAS collaboration (2013)]

Neutrinos	$p_{\mathrm{T}}^{\nu\bar{\nu}} > 90\,\mathrm{GeV}$
Photon	$p_{\mathrm{T}}^{\gamma} > 100\,\mathrm{GeV}$ $\lvert\eta^{\gamma}\rvert < 2.37$ Frixione isolation with $\varepsilon_{\gamma} = 0.5,\ R = 0.4,\ n = 1$
Jets	$p_{\mathrm{T}}^{\mathrm{jet}} > 30\,\mathrm{GeV}$ $\lvert\eta^{\mathrm{jet}}\rvert < 4.4$ $N_{\mathrm{jet}} \geq 0$ (inclusive) or $N_{\mathrm{jet}} = 0$ (exclusive)
Separation	$\Delta R(\gamma, \mathrm{jet}) > 0.3$

LO diagrams